Fixture Failure Diagnosis for Autobody Assembly Using Pattern Recognition

D. Ceglarek

J. Shi

S. M. Wu Manufacturing Research Center,
Department of Mechanical Engineering
and Applied Mechanics,
The University of Michigan, Ann Arbor, MI
48109-2125

In this paper, a fault diagnostic method is proposed for autobody assembly fixtures. This method uses measurement data to detect and isolate dimensional faults of part caused by fixture. The proposed method includes a predetermined variation pattern model and a fault mapping procedure. The variation pattern model is based on CAD information about the fixture geometry and location of the measurement points. This fault mapping procedure combines Principal Component Analysis with pattern recognition approach. Simulations and one case study illustrate the proposed method.

1 Introduction

Autobody assembly is a very complex process. It requires dozens of fixtures to assemble on average 150–250 parts. The complexity of the assembly line puts high demands on the tooling fixtures. Therefore, design, manufacture, and diagnosis of fixtures are important issues for improving autobody quality.

In recent years, fixture modeling and design have been thoroughly studied and significant results have been achieved (Asada and By, 1985; Chou et al., 1989; Menassa and De Vries, 1989). Fixture designs are analyzed in terms of their ability to arrest translation and rotation, while minimizing deflection and distortion of the part during processing (Chou et al., 1989). Kinematical and mechanical methods such as screw theory (Asada and By, 1985) and force equilibrium equations (Salisbury and Roth, 1983) are most often used for functional configuration of the fixture. Menassa and De Vries presented a synthesis of this approach (1989). Although such advances in fixture design can greatly improve fixture accuracy and repeatability, fixture faults are still the major root cause of autobody dimensional variation (ABC, 1993). However, there is very little literature investigating fixture diagnosis based on the dimensional variation of parts.

In recent years, the implementation of the in-line Optical Coordinate Measurement Machine (OCMM) in the automotive industry provides new opportunities for fixture fault diagnosis. OCMM gages are installed at the end of major assembly processes, such as framing, side frames, underbody, etc. The OCMM measures 100 to 150 points on each major assembly with a 100 percent sample rate. These inspected points are located on each individual part of the autobody. As a result, the OCMM provides tremendous amounts of dimensional information, which can be used for assembly process control. However, effective implementation of this measurement information, especially for fixture fault diagnosis, is still a challenge. These challenges can be summarized as:

(1) *Sensor synthesis in the dimensional analysis:* Fixture diagnosis requires identifying and describing the variation pattern of a part orientation and position. Identification can be achieved by dimensional sensors, which are highly suitable for part position and orientation checks (Tlusty and Andrews, 1983). However, no single sensor can describe the variation pattern of a part. Additionally, there is no model which relates the variation pattern to sensor readings. Thus, sensor synthesis using advanced statistics has to be applied in this development.

(2) *Engineering interpretation of the multi-dimensional measurements:* Historically, dimensional analysis of the assembly line began by using statistical techniques to assign quality targets to isolate faults off-line (Takezawa, 1980). Takezawa (1980) examined the addition theorem of variances to establish dimensional relationships between subassemblies. Besides his contributions, most of the monitoring methods for manufacturing processes are based on statistical techniques such as Statistical Process Control (SPC). Statistical techniques have not been widely used for on-line evaluation of faults in quality systems (Faltin and Tucker, 1991). Hu and Wu (1992) as well as Roan et al. (1993) presented an intuitive interpretation of the dimensional faults detected by multidimensional measurements and represented in the form of variation patterns. However, there is no generic and proven approach linking patterns of dimensional variation with fault root causes.

(3) *Integration of advanced statistics and engineering knowledge for root cause identification:* Pure statistical methods, without integration with knowledge about the product/process, are not sufficient to identify the root cause of the fault. Schwarz and Lu (1992) emphasized the integration of statistical methods with knowledge-based techniques to provide enhanced decision support capabilities. Dessouky et al. (1987) successfully applied decision tree analysis, supported by time series modeling to diagnose process quality. Integration of knowledge with statistics is especially important during dimensional diagnosis of a multi-fixture system such as an autobody assembly. However, no approach currently models assembly fixtures for diagnostic purposes.

In recent years, research exploring fault isolation issues in autobody assembly has focused on the statistical descriptions of variation patterns (Hu and Wu, 1992) and the detection of failing assembly stations (Ceglarek et al., 1994). Hu and Wu (1992) investigated the description of the dimensional faults by in-line measurement data using Principal Component Analysis (PCA). Ceglarek et al. (1994) described a systematic method of identifying failing stations and faulty parts in the assembly line. Additionally, they described a rule-based approach to identify root causes of dimensional faults in the fixture. Their rule-based approach is based on heuristic knowledge which specifies a fixed level of detail about the position and control directions of the fixture locators.

This paper attempts to resolve the above mentioned challenges by developing a fixture fault diagnostic approach which integrates in-line dimensional measurements, advanced statistics, product and fixture design as well as pattern recognition. The selection of fixture failures was based on an investigation of the most severe faults occurring during the 18-month development cycle of a domestic sport utility vehicle. The study

Contributed by the Manufacturing Engineering Division for publication in the JOURNAL OF ENGINEERING FOR INDUSTRY. Manuscript received Dec. 1993; revised Aug. 1994. Technical Editor: S. Kapoor.

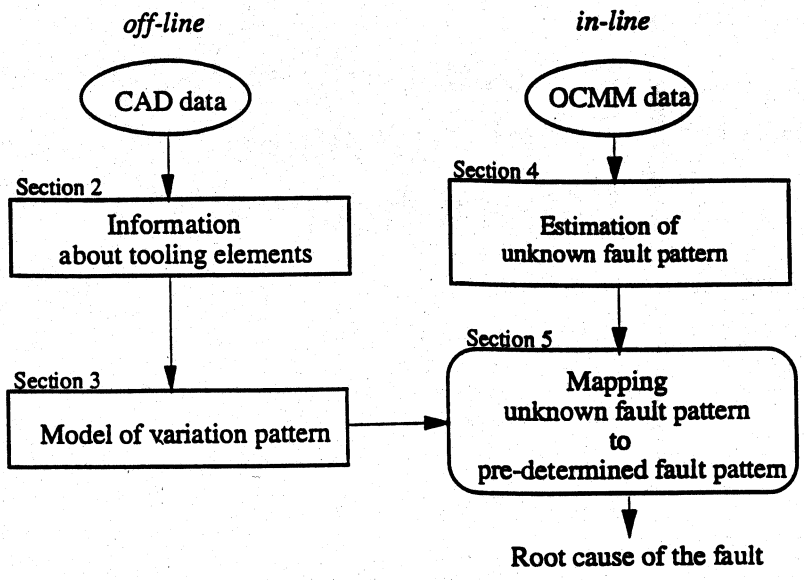

Fig. 1 Outline of the method

started at pilot phase and was conducted until 2-shift full production phase. During the study, 52 case studies with 118 root causes were identified and solved (Ceglarek et al., 1993, Ceglarek and Shi, 1995). The conclusion from this investigation was that 72 percent of all root causes were due to fixture failures (Ceglarek et al., 1993; Ceglarek, 1994).

The proposed method is presented in three parts. The first part, develops a variation pattern model for each hypothetical fault derived, based on the CAD data for the fixture (Sections 2 and 3). The model of the variation pattern is based solely on the fixture configuration and measurement location. The relation between layout of tooling elements and measurements are developed and used for modeling the fault variation pattern. Additionally, hypothetical tooling faults as well as their manifestations through dimensional sensors are thoroughly discussed. Part one of the paper develops a variation pattern model based solely on the engineering knowledge stored in the CAD system (fixture geometry—position of all locators; measurement information—position of all measurement points). In the second part of the paper, a variation pattern for an unknown fault is described based on the multisensor data, solely through a multivariate statistical approach—Principal Component Analysis. (Section 4). The relationship between parts one and two (engineering knowledge—statistical knowledge) is discussed in part three of the paper. The third part of the paper maps the model of the variation pattern (engineering knowledge) with the variation pattern of an unknown fault (statistical knowledge) using a pattern recognition approach (Section 5). Fault mapping includes two tasks: (1) estimating the dominant direction of the fault variation pattern, and (2) isolating the fault of the dominant direction using a minimum distance classifier. A minimum distance classifier determines the unknown fault based on its distance from the predetermined variation pattern described in the model. The outline of these two parts is shown in Fig. 1. The third part of the paper illustrates and verifies the proposed method through a series of computer simulations (Section 7) and one case study based on the production data (Section 8).

2 Autobody Part Fixture and Its Hypothetical Faults

This section presents an investigation of autobody parts and assembly fixtures. Relations between hypothetical faults and fixture geometry, based on in-line measurements, are studied. These relations are used during development of the variation pattern model.

2.1 Autobody Part. An autobody is built of sheet metal parts which have different shapes, sizes and thicknesses, depending on their functions. The parts are divided into structural and non-structural parts. Structural parts support the autobody structure as (1) main parts, for example rails and plenum, or as (2) reinforcement parts, for instance door hinge reinforcements. The other parts are called nonstructural parts, for example, door outer, cowlside, roof and so on.

Structural parts are usually much more rigid than nonstructural parts, and usually have a much bigger impact on the autobody dimensional accuracy (ABC, 1993). Similar conclusions were made by Takezawa (1980). Based on his study, he concluded that the parts with low rigidity fit into the final assembly with little dimensional influence. Thus, the detection of dimensional faults affecting structural parts addressed in this paper, is critical for the assembly process.

2.2 Fixture Layout for a Rigid Part. As in machining, an assembly fixture must satisfy the following four conditions for holding parts (Chou et al., 1989): locating stability, clamping stability, deterministic part location, and total restraint. These conditions impact on the dimensional variation of the product. Locating stability and deterministic part location are specified by correct layout of the locators (typically locating pins and *NC* locators). Clamping stability is defined by location and closing sequence of the clamps. Asada and By (1985) showed mathematical relations for these conditions.

The results presented by Asada and By (1985) and Chou et al. (1989) show that satisfying the aforementioned conditions is sufficient to have a correct fixture. These conditions are realized directly through locating pins (P) and *NC* blocks ($C = NC$ locator + clamp). Therefore, we assume that Ps and Cs have primary responsibilities for fixture function, and therefore for product dimensional variation.

Based on this assumption, Ps and Cs are selected as the major elements of the fixture contributing to the variation of the product. From the discussion in Section 2.1, which concluded that structural parts have the greatest impact on the variation, we will focus our analysis on fixture fault diagnosis for rigid parts. For a rigid part, the most common layout method is the 3-2-1 principle. The 3-2-1 principle locates a part by three groups of locators laid out in two orthogonal planes. As shown in Fig. 2 these three groups usually include: (1) a four-way (expanding or stationary) pin P_1 to precisely position the part in two directions (X and Z) on the first plane, (2) a two-way

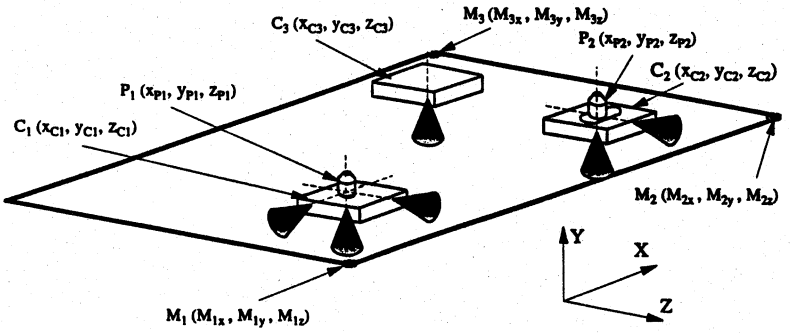

Fig. 2 A layout of *3-2-1* fixture with marked *Ps*, *Cs* and *Ms* points

pin P_1 or *NC* block to locate the part in one direction (Z) laid in the first plane, and (3) all remaining *NC* locators (C_1, C_2, C_3) to locate the part in the second plane (Y direction).

2.3 Hypothesis of Fixture Faults. The hypotheses of tooling faults are derived from the *3-2-1* layout fixture. The basic set of potential tooling faults which could contribute to dimensional variation is prefixed and limited to the major elements of the fixture. This paper addresses the issue of faults caused by fixture locator malfunction.

Definition 1. A set of Pin Locating Points (*Ps*) and *NC* block Locating Points (*Cs*) in the given fixture is called a *Set of Tooling Elements.* Each element of that set is called a *Tooling Element* (TE).

Ceglarek et al. (1994) lists examples of faults related to the TEs. In this paper the tooling element (TE) faults are understood as any tooling discrepancies that cause part mislocation in the final product. Faults of the TE can be caused by locator wear, inclusions on the locating surface of locators, or clamps that do not properly force the part against the locator. Furthermore, each TE has a part control axis, which defines the critical direction for that given TE. For example, the part control axis of the locating pin P_2 (Fig. 2) is the Z axis. Faults caused by failure of the TEs manifest themselves in a specific predetermined way. These manifestations can be described by measurements, and information about sensor location, which are as follows:

Definition 2. Set of Complement Tooling Elements (CTE) to a specified tooling element TE in the given axis Ξ, is a subset of all tooling elements which control the part in the Ξ axis, except the tooling element TE.

Corollary 1. Failure of the *Tooling Element* TE, which controls part in the Ξ axis, causes mislocation of the part according to the rigid motion, defined by the all *Complement Tooling Elements* (CTEs) to element TE in the Ξ axis.

Proof. In order, for a part to be detachable from the desired location on the fixture, there must exist at least one admissible motion called part mislocation which is caused by failure of a tooling element, for example TE. Since TE controls only the Ξ axis, the failure of this element might cause dimensional discrepancies of the part only in that axis. Additionally, the part is controlled in the Ξ axis only by complement tooling elements to TE. Therefore, the dimensional mislocation of the part is determined by the configuration of the CTE. The proposition that the part is mislocated in the sense of rigid motion, is based on the design principle for the *3-2-1* layout fixture, which assumes no deformation of the part in the fixture. ■

Theorem 1. Motion of the mislocated part, due to failure of a tooling element TE which controls the part in the Ξ axis, can be described as:

(1) translation along the Ξ axis,
if the number of complement tooling elements to TE, $n_{CTE} = 0$;

(2) rotation along the axis defined by one complement tooling element,
if the number of complement tooling elements to TE, $n_{CTE} = 1$;

(3) rotation along the axis defined by two complement tooling elements,
if the number of complement tooling elements to TE, $n_{CTE} = 2$.

Table 1 summarizes the fault manifestations described by *Corollary* 1 and *Theorem* 1. Arrows in Table 1 represent the direction of part mislocation due to the TE failure.

3 Representation of Dimensional Faults

This section investigates the geometrical relations in tooling fixtures and analyzes the hypothetical faults which might occur. The main goal of this section is to derive a generic model of variation patterns for the failure of each TE. The model describes the relationship between the in-line measurements obtained from OCMM gages under single failure condition. The OCMM gages are installed at the end of major assembly processes, such as framing, side frames, underbody, etc. The OCMMs are used to measure dimensions of automotive bodies relative to design nominals. All OCMM gages in the plant use the same coordinate system, called the body coordinate system,

Table 1 Manifestation of a single fault

Fault	Fault manifestation	n_{CTE}
P_1	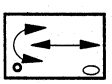	X 0 Z 1
P_2	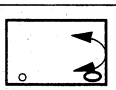	1
C_1	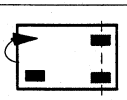	2
C_2	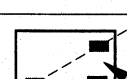	2
C_3	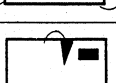	2

which makes it easy to use and compare data from different gages. Additionally, the same coordinate system is used during product and tooling design.

3.1 The Relationship between Fixture Geometry and Dimensional Variation. Fixture layout obtained from CAD is important information for dimensional diagnosis. Figure 2 shows the location of the TEs in Cartesian coordinates. The manifestation of the TE faults is represented by sensors M_i (M_{ix}, M_{iy}, M_{iz}) and their standard deviations $\sigma_i(\sigma_{ix}, \sigma_{iy}, \sigma_{iz})$, $i = 1, 2, 3$. Total variation of each sensor can be decomposed into the variation along the individual directions as follows:

$$(\sigma_i)^2 = (\sigma_{ix})^2 + (\sigma_{iy})^2 + (\sigma_{iz})^2 \quad i = 1, 2, 3 \qquad (1)$$

The magnitude of dimensional variation captured by sensors depends on the severity of the fault, described by the standard deviation of the TE, σ^F_{TE}, as well as on the geometrical relations between the location of the sensors and the TEs. These relations are presented by *Theorem* 2 as follows:

Theorem 2. Relations between fixture geometry and dimensional variation, during failure of the tooling element TE, is described by measurement data from sensors M_1, M_2, M_3 as follows:

(1) in case the number of complement tooling elements $n_{\mathrm{CTE}} = 0$

$$\sigma^F_{\mathrm{TE}} = \sigma_1 = \sigma_2 = \sigma_3 \qquad (2)$$

(2) in case the number of complement tooling elements $n_{\mathrm{CTE}} = 1$

$$\frac{\sigma^F_{\mathrm{TE}}}{d(\mathrm{TE}, \mathrm{CTE})} = \frac{\sigma_1}{d(\mathrm{CTE}, M_1)} = \frac{\sigma_2}{d(\mathrm{CTE}, M_2)} = \frac{\sigma_3}{d(\mathrm{CTE}, M_3)} \qquad (3)$$

where $d(a, b)$ is a Euclidean distance between point a and b defined as:

$$d(a, b) = \sqrt{(x_a - x_b)^2 + (y_a - y_b)^2 + (z_a - z_b)^2} \qquad (4)$$

(3) in case the number of complement tooling elements $n_{\mathrm{CTE}} = 2$

$$\frac{\sigma^F_{\mathrm{TE}}}{d(\mathrm{TE}, \mathrm{CTE}_{12})} = \frac{\sigma_1}{d(\mathrm{CTE}_{12}, M_1)} = \frac{\sigma_2}{d(\mathrm{CTE}_{12}, M_2)} = \frac{\sigma_3}{d(\mathrm{CTE}_{12}, M_3)} \qquad (5)$$

where CTE_{12} is an axis between complement tooling elements 1 and 2.

Proof. The proof for Eq. (3) is conducted. Equations (2) and (5) can be proved following the same procedure. Let M_1, M_2, M_3 and M_1', M_2', M_3' be the points located on the part before and after rotation of that part respectively (Fig. 3). And let δ_1, δ_2, δ_3 describe the distance of each point M_1, M_2, M_3 from the center of rotation O. Simultaneously ξ_i is the distance between points M_i and M_i' points $(i = 1, 2, 3)$.

First, observe that in general $\xi_1/\delta_1 = \xi_2/\delta_2 = \xi_3/\delta_3$, holds for rotation of the part, so this relation can be rearranged as:

$$\xi_{i+1} = \frac{\delta_{i+1}}{\delta_i}\xi_i = \kappa_i\xi_i \quad \text{for} \quad i = 1, 2 \qquad (6)$$

where $\kappa_i = \delta_{i+1}/\delta_i$ is a constant. The standard deviation of point M_i can be calculated as:

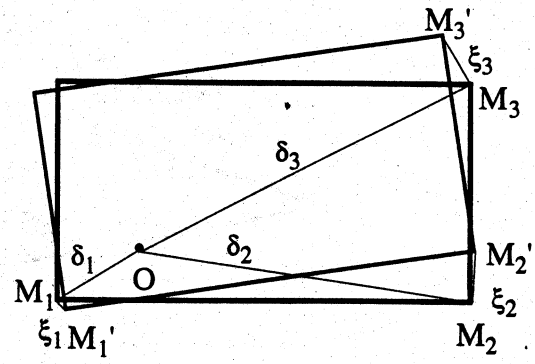

Fig. 3 Geometrical relations during rotation of the rigid part

$$\sigma_i = \sqrt{\frac{\sum_{j=1}^{N}((\xi_i)_j - \bar{\xi}_i)^2}{N-1}} \qquad (7)$$

where $\bar{\xi}_i$ is the mean dislocation of the point M_i, $i = 1, 2, 3$, and N is the sample size. Substituting Eq. (6) to Eq. (7), we obtain the following:

$$\sigma_{i+1} = \sqrt{\frac{\sum_{j=1}^{N}((\kappa_i\xi_i)_j - \overline{\kappa_i\xi_i})^2}{N-1}} = \kappa_i\sqrt{\frac{\sum_{j=1}^{N}((\xi_i)_j - \bar{\xi}_i)^2}{N-1}} = \kappa_i\sigma_i \qquad (8)$$

Equation (8) defines the relationship between variation σ_i and geometric parameter κ_i, $i = 1, 2, 3$. Thus:

$$\frac{\sigma_3}{\delta_3} = \frac{\sigma_2}{\delta_2} = \frac{\sigma_1}{\delta_1} = \frac{\sigma_0}{\delta_0} \qquad (9)$$

For $n_{\mathrm{CTE}} = 1$, let point O (Fig. 3) shows the location of the CTE, and standard deviations σ_0, σ_1, σ_2, σ_3 represent variation of the TE, and measurement sensors M_1, M_2, M_3 respectively. Thus, the distances δ_0, δ_1, δ_2, δ_3 represent $d(\mathrm{CTE}, \mathrm{TE})$, $d(\mathrm{CTE}, M_1)$, $d(\mathrm{CTE}, M_2)$, and $d(\mathrm{CTE}, M_3)$ respectively. Substituting the aforementioned relations into Eq. (9), we get Eq. (3). ■

Theorem 2 extends the linear relation between the motion of the points located on the rigid part during rotation of that part (Paul, 1981), to the linear relations between the variances of those points and their locations. In order to illustrate the use of *Theorem* 2, a failure of P_2 is explained in the following example.

Example—Failure of P_2. Tooling element P_2 controls part motion in the Z axis (Fig. 4). There are two TEs controlling motion along the Z axis: pins P_1 and P_2. Thus, based on *Definition 2,* pin P_1 is the only CTE to P_2 in the Z axis ($n_{\mathrm{CTE}} = 1$). Further, based on part (2) of Theorem 1, the fault at P_2 can be represented as a rotation of the part around P_1 (Fig. 4). Based on Eq. (3) of *Theorem* 2, it can be quantitatively described as:

$$\frac{\sigma^F_{P2}}{d(P_2, P_1)} = \frac{\sigma_1}{d(P_1, M_1)} = \frac{\sigma_2}{d(P_1, M_2)} = \frac{\sigma_3}{d(P_1, M_3)} \qquad (10)$$

The fault at P_2 is represented in Fig. 4 as a standard deviation σ^F_{P2}.

3.2 Model of the Variation Pattern for *3-2-1* Layout Fixture. The model of the *3-2-1* layout fixture describes the part variation pattern in terms of the TEs and measurement layout. Sensor layout in the fixture uses 9 variables (3 sensors measuring 3 axes each) to describe the *3-2-1* fixture. In order to formal-

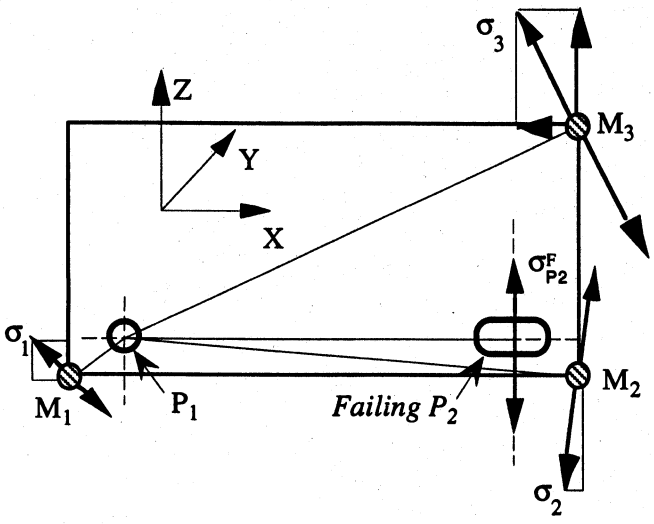

Fig. 4 Geometrical interpretation of the failing locator P_2

ize the relationship between faults of the TEs and fixture geometry, the following definitions are proposed:

Definition 3. Fixture faults caused by a TE malfunction are classified as follows:

Type-1 fault: failing pin P_1 in Z axis
Type-2 fault: failing pin P_1 in X axis
Type-3 fault: failing pin P_2 in Z axis
Type-4 fault: failing NC block C_1 in Y axis
Type-5 fault: failing NC block C_2 in Y axis
Type-6 fault: failing NC block C_3 in Y axis

Definition 4. A diagnostic vector $d(i) = (d_{1i}, \ldots, d_{ni})^T$ has n entries corresponding to the measured variables χ_j describing a variation pattern caused by type-i fault, with

$$d_{ji} = \frac{\sigma_{\chi_j}}{\sigma} \quad j = 1, \ldots, n \tag{11}$$

where σ_{χ_j} is a standard deviation of variable χ_j, and $\sigma = \sqrt{\sum_{j=1}^{n} \sigma_{\chi_j}^2}$, where n is the number of measured variables.

Theorem 3. The model of the variation pattern for the *3-2-1* fixture is described by diagnostic matrix $\mathbf{D} = (\mathbf{d}(1), \ldots, \mathbf{d}(6))$. The ith column of the $\mathbf{D}$ matrix is the diagnostic vector $\mathbf{d}(i)$ $(i = 1, \ldots, 6)$, corresponding to type-i fault.

$$\mathbf{D} = \begin{bmatrix} d_{11} & d_{12} & \cdots & d_{16} \\ d_{21} & d_{22} & \cdots & d_{26} \\ \cdots & \cdots & \cdots & \cdots \\ d_{n1} & a_{n2} & \cdots & d_{n6} \end{bmatrix} \tag{12}$$

where elements d_{ji} for $j = 1, \ldots n$ and $i = 1, \ldots 6$, are shown in Table 2.

Proof. This paper conducts proofs for vectors $\mathbf{d}(1)$, $\mathbf{d}(2)$ and $\mathbf{d}(4)$. The other diagnostic vectors can be derived in a similar manner. In the case of the *3-2-1* fixture (Fig. 4), a measurement vector χ based on sensors M_i $(i = 1, 2, 3)$ is defined as:

$$\chi = [\chi_1, \chi_2, \chi_3, \chi_4, \chi_5, \chi_6, \chi_7, \chi_8, \chi_9]^T$$
$$= [M_{1x}, M_{1y}, M_{1z}, M_{2x}, M_{2y}, M_{2z}, M_{3x}, M_{3y}, M_{3z}]^T \tag{13}$$

Type-1 fault: failing P_1 in Z axis. Diagnostic vector $\mathbf{d}(1)$ is determined based on the measurement vector and describes the variation pattern of type-1 fault. Diagnostic vector $\mathbf{d}(1)$ is defined from Eq. (11) as:

$$d_{j1} = \frac{\sigma_{\chi_j}}{\sigma} \quad \text{for} \quad j = 1, 3, 4, 6, 7, 9 \quad \text{and}$$

$$d_{j1} = 0, \quad \text{for} \quad j = 2, 5, 8 \tag{14}$$

Based on Eq. (3) from *Theorem* 2

$$\sigma_j = \sigma_{P1}^F \frac{d(P_2, M_j)}{d(P_2, P_1)}, \quad j = 1, 2, 3 \tag{15}$$

Additionally from Fig. 4 and *Theorem* 2

$$\frac{\sigma_{\chi_{(3j-2)}}}{\sigma_j} = \frac{z(P_2, M_j)}{d(P_2, M_j)}, \quad \frac{\sigma_{\chi_{(3j)}}}{\sigma_j} = \frac{x(P_2, M_j)}{d(P_2, M_j)}, \quad j = 1, 2, 3 \tag{16}$$

where $z(P_2, M_j)$ is the distance in the Z direction from pin P_2 to sensor M_j (Fig. 2), $x(P_2, M_j)$ is the distance in the X direction from pin P_2 to sensor M_j, and σ_j is the total standard deviation calculated for the jth sensor. Substituting Eqs. (16) to Eq. (15):

$$\sigma_{\chi_{(3j-2)}} = \sigma_{P1}^F \frac{z(P_2, M_j)}{d(P_2, P_1)},$$

$$\sigma_{\chi_{(3j)}} = \sigma_{P1}^F \frac{x(P_2, M_j)}{d(P_2, P_1)} \quad j = 1, 2, 3 \tag{17}$$

Total standard deviation in the data is calculated as follows:

$$\sigma = \sqrt{\sigma_1^2 + \sigma_2^2 + \sigma_3^2}$$
$$= \sigma_{P1}^F \frac{\sqrt{d^2(P_2, M_1) + d^2(P_2, M_2) + d^2(P_2, M_3)}}{d(P_2, P_1)} \tag{18}$$

Thus, substituting Eqs. (18) and (17) to Eq. (14) diagnostic vector $\mathbf{d}(1)$ can be presented in the following form:

$$\mathbf{d}(1) = \frac{[z(P_2M_1) \quad 0 \quad x(P_2, M_1) \quad z(P_2, M_2) \quad 0 \quad x(P_2, M_2) \quad z(P_2, M_3) \quad 0 \quad x(P_2, M_3)]^T}{\sqrt{d^2(P_2, M_1) + d^2(P_2, M_2) + d^2(P_2, M_3)}} \tag{19}$$

The diagnostic vector $\mathbf{d}(1)$ is represented as the first column in Table 2.

Type-2 fault: failing P_1 in X axis. Type-2 fault describes failing pin P_1 in the X axis alone. Therefore, diagnostic vector $\mathbf{d}(2)$ is determined from Eq. (11) as:

$$d_{j2} = \frac{\sigma_{\chi_j}}{\sigma} \quad \text{for} \quad j = 1, 4, 7 \quad \text{and}$$

$$d_{j2} = 0 \quad \text{for} \quad j = 2, 3, 5, 6, 8, 9 \tag{20}$$

Based on Eq. (2) of *Theorem* 2

$$\sigma_{P1}^F = \sigma_1 = \sigma_2 = \sigma_3 \tag{21}$$

and

$$\sigma_{P1}^F = \sigma_{\chi_1} = \sigma_{\chi_4} = \sigma_{\chi_7} \quad \text{and}$$

$$\sigma_{\chi_j} = 0 \quad j = 2, 3, 5, 6, 8, 9 \tag{22}$$

Additionally, the total standard deviation in the data is equal to

$$\sigma = \sqrt{\sum_j \sigma_j^2} = \sqrt{3}\sigma_{P1}^F \quad j = 1, 4, 7 \tag{23}$$

Table 2 Model of variation pattern for *3-2-1* layout fixture

element \ vector	d(1)	d(2)	d(3)	d(4)	d(5)	d(6)
1	$\frac{z(P_2,M_1)}{\mathcal{A}}$	0.577	$\frac{z(P_1,M_1)}{\mathcal{B}}$	0	0	0
2	0	0	0	$\frac{d(C_{23},M_1)}{C_1}$	$\frac{d(C_{13},M_1)}{C_2}$	$\frac{d(C_{12},M_1)}{C_3}$
3	$\frac{x(P_2,M_1)}{\mathcal{A}}$	0	$\frac{x(P_1,M_1)}{\mathcal{B}}$	0	0	0
4	$\frac{z(P_2,M_2)}{\mathcal{A}}$	0.577	$\frac{z(P_1,M_2)}{\mathcal{B}}$	0	0	0
5	0	0	0	$\frac{d(C_{23},M_2)}{C_1}$	$\frac{d(C_{13},M_2)}{C_2}$	$\frac{d(C_{12},M_2)}{C_3}$
6	$\frac{x(P_2,M_2)}{\mathcal{A}}$	0	$\frac{x(P_1,M_2)}{\mathcal{B}}$	0	0	0
7	$\frac{z(P_2,M_3)}{\mathcal{A}}$	0.577	$\frac{z(P_1,M_3)}{\mathcal{B}}$	0	0	0
8	0	0	0	$\frac{d(C_{23},M_3)}{C_1}$	$\frac{d(C_{13},M_3)}{C_2}$	$\frac{d(C_{12},M_3)}{C_3}$
9	$\frac{x(P_2,M_3)}{\mathcal{A}}$	0	$\frac{x(P_1,M_3)}{\mathcal{B}}$	0	0	0

where $\mathcal{A}=\sqrt{d^2(P_2,M_1)+d^2(P_2,M_2)+d^2(P_2,M_3)}$;

$\mathcal{B}=\sqrt{d^2(P_1,M_1)+d^2(P_1,M_2)+d^2(P_1,M_3)}$;

$C_1=\sqrt{d^2(C_{23},M_1)+d^2(C_{23},M_2)+d^2(C_{23},M_3)}$;

$C_2=\sqrt{d^2(C_{13},M_1)+d^2(C_{13},M_2)+d^2(C_{13},M_3)}$;

$C_3=\sqrt{d^2(C_{12},M_1)+d^2(C_{12},M_2)+d^2(C_{12},M_3)}$

Substituting Eqs. (23) and (22) to Eq. (20) diagnostic vector $\mathbf{d}(1)$ can be presented as:

$$\mathbf{d}(2) = 0.577[1 \quad 0 \quad 0 \quad 1 \quad 0 \quad 0 \quad 1 \quad 0 \quad 0]^T \quad (24)$$

The diagnostic vector $\mathbf{d}(2)$ is represented as the second column in Table 2.

Type-4 fault: failing C_1 in Y axis. Type-4 fault describes failing pin C_1 in the Y axis alone. Therefore, diagnostic vector $\mathbf{d}(4)$ is determined from Eq. (11) as:

$$\mathbf{d}(4) = \frac{[0 \quad d(C_{23}, M_1) \quad 0 \quad 0 \quad d(C_{23}, M_2) \quad 0 \quad 0 \quad d(C_{23}, M_3) \quad 0]^T}{\sqrt{d^2(C_{23}, M_1) + d^2(C_{23}, M_2) + d^2(C_{23}, M_3)}} \quad (29)$$

$d_{j4} = \frac{\sigma_{x_i}}{\sigma}$ for $j = 2, 5, 8$ and

$$d_{j4} = 0 \quad \text{for} \quad j = 1, 3, 4, 6, 7, 9 \quad (25)$$

Based on Eq. (5) in *Theorem* 2

$$\sigma_j = \sigma_{C1}^F \frac{d(C_{23}, M_j)}{d(C_{23}, C_1)}, \quad j = 1, 2, 3 \quad (26)$$

and

$\sigma_{x_1} = \sigma_1$; $\sigma_{x_4} = \sigma_2$; $\sigma_{x_7} = \sigma_3$ and

$$\sigma_{x_j} = 0 \quad j = 2, 3, 5, 6, 8, 9 \quad (27)$$

Additionally the total standard deviation in the data is calculated as

$$\sigma = \sqrt{\sum_{j=1}^{3} \sigma_j^2} = \sigma_{C1}^F \frac{\sqrt{d^2(C_{23}, M_1) + d^2(C_{23}, M_2) + d^2(C_{23}, M_3)}}{d(C_{23}, C_1)} \quad (28)$$

where $d(C_{ij}, M_k)$ is the Euclidean distance from the axis defined by NC blocks C_i and C_j to the sensor M_k (Fig. 2). Finally, diagnostic vector $d(4)$ can be presented in the following form:

The diagnostic vector $\mathbf{d}(4)$ is represented as the fourth column in Table 2. ■

Each diagnostic vector represents a variation pattern of one fault defined in *Definition* 2. Results from Table 2 show that elements of all diagnostic vectors depend on the geometry of the fixture, i.e., location of the TEs and sensors.

4 Description of Variation Pattern Using Principal Component Analysis (PCA)

4.1 Principle Component Analysis (PCA). The variation pattern of a single part is estimated based on PCA (Hu and Wu, 1992). In PCA, the goal is to model one sample of data using orthogonal components. PCA linearly transforms an

original set of variables into a set of uncorrelated variables that represents most of the information in the original set of variables. The number of principal components is equal to the dimensionality of the variable space (Jolliffe, 1986).

In the case of autobody diagnosis without noise, the dimensionality of the variable space is equal to the number of faults. PCA describes a variation pattern by finding $p \leq n$ linear transformations of n variables. Each variable represents measurement data from one of three sensors (M_1, M_2 and M_3) in one axis (X, Y or Z), i.e., $n = 9$.

Let $\chi \in R^n$, represent N measurements from n sensors with covariance matrix $\mathbf{Q} = E(\chi\chi^T)$. Define $\tilde{\chi} \in R^p$ for $p \leq n$, as a transformation of χ such that

$$\tilde{\chi}_i = A\chi_i \quad i = 1, \ldots, n \tag{30}$$

where $\mathbf{A} = [a_{ij}]_{n\times n}$. The ith column of $\mathbf{A}$ represented as $\mathbf{a}_i = [a_{i1}, \ldots, a_{in}]^T$, is the ith eigenvector of the covariance matrix Σ obtained in the form

$$[\lambda_i \mathbf{I} - \mathbf{Q}]\mathbf{a}_i = 0, \quad i = 1, \ldots, n \tag{31}$$

where λ_i is the eigenvalue of the ith principal component, $\mathbf{I}$ is the identity matrix and a_i is the ith eigenvector corresponding to λ_i. The detailed procedure of the PCA can be found in Jolliffe (1986). In the case of the *3-2-1* fixture (Fig. 4), principal components are a linear combination of the $n = 9$ variables defined in Eq. (13).

The ith principal component a_i maximizes the variance of $\sum_{j=1}^{9} (a_{ij}\chi_j)$ given that $\sum_{j=1}^{9} a_{ij}^2 = 1$, and that this component is linearly independent of all prior principal components.

The sum of sample variances of the principal components is equal to the sum of variances of the original variables $\sigma_i^2 = \text{var}(\chi_i)$

$$\sum_{i=1}^{9} \sigma_i^2 = \sum_{i=1}^{9} \lambda_i = \text{trace}(\mathbf{Q}) \tag{32}$$

Based on the variance properties (Morrison, 1967) this relation can be reformulated as:

$$\lambda_i = \sum_{j=1}^{9} \text{var}(\tilde{\chi}_j) = \sum_{j=1}^{9} \text{var}(a_{ij}\chi_j) \tag{33}$$

Knowing that component a_{ij} is constant for a given variation pattern, and applying again the variance property

$$\lambda_i = \sum_{j=1}^{9} a_{ij}^2 \,\text{var}(\chi_j) \tag{34}$$

Vectors $\mathbf{a}_i^T = (a_{i1}, \ldots, a_{i9})$, $i = 1, \ldots, 9$ represent variation patterns. Coefficient a_{ij} can be interpreted as a weight assigned to the ith mode by the jth variable. Geometrically, the first eigenvector points in the direction of the greatest variability in the data, and the orthogonal projection of the data onto this eigenvector is the first eigenvalue.

4.2 The Relationship between Variation Pattern Model of the *3-2-1* Fixture and PCA. The relations between fixture geometry, dimensional variation and faults are summarized as Theorem 3. In this section, based on *Theorem* 3 and PCA, relations between variation pattern, represented by diagnostic vector $\mathbf{d}(i)$, and the principal component $\mathbf{a}_1$, represented as the first eigenvector in Eq. (31), are derived. These relations are presented in the form of the following theorems.

Lemma. A single fault, defined in *Definition 3,* is manifested through a variation pattern, modeled and based on the measurements from sensors M_1, M_2, M_3, and described by one eigenvector-eigenvalue pair $(\mathbf{a}_1, \lambda_1)$.

Proof. The total standard deviation in the data caused by a single fault derived from fixture geometry can be expressed in the same form as the variation described by one eigenvector.

Based on Theorem 2, for any single TE fault, there exist constants, $j = 1, 2, 3$ such that

$$\sigma_j = k_j' \sigma_{\text{TE}}^F \tag{35}$$

For example, for a type-1 fault, $k_j' = d(P_2, M_j)/d(P_1, P_2)$. From Eq. (16)

$$\sigma_{\chi_i} = k_i'' \sigma_1, \quad i = 1, 2, 3; \quad \sigma_{\chi_i} = k_i'' \sigma_2, \quad i = 4, 5, 6;$$

$$\sigma_{\chi_i} = k_i'' \sigma_3, \quad i = 7, 8, 9 \tag{36}$$

where k_i'' are constant. In case of a type-1 fault, k_i'' is equal to: $k''_{(3j-2)} = z(P_2, M_j)/d(P_2, M_j)$, $k''_{(3j-1)} = 0$, $k''_{(3j)} = x(P_2, M_j)/d(P_2, M_j)$, for $j = 1, 2, 3$.

Substituting Eq. (35) to Eq. (36), one can get

$$\sigma_{\chi_i} = k_i \sigma_{\text{TE}}^F, \quad i = 1, \ldots, 9 \tag{37}$$

where $k_i = k_i' k_i''$ are constants. Total standard deviation in the data σ caused by the fault is equal to

$$\sigma = \sqrt{\sum_{i=1}^{9} \sigma_{\chi_i}^2} = \sqrt{\sum_{i=1}^{9} k_i^2 (\sigma_{\text{TE}}^F)^2} = \sigma_{\text{TE}}^F \sqrt{\sum_{i=1}^{9} k_i^2} \tag{38}$$

where σ_{TE}^F is a variable referred to as the standard deviation of the TE fault.

On the other hand, Eq. (34) defines relations between the eigenvectors and the eigenvalues. In the situation when only one eigenvalue exists, Eq. (34) is equal to

$$\sigma^2 = \lambda_1 = \sum_{j=1}^{9} a_{1j}^2 \,\text{var}(\chi_j) \tag{39}$$

which is equivalent to Eq. (38), for $\text{var}(\chi_j) = \sigma_{\text{TE}}^F$, and $k_i = a_{1i}$ $(i = 1, \ldots, 9)$. Knowing that the first eigenvector describes the maximum variance expressed using linear components $a_{11}, \ldots, a_{19}$, it can be stated that the variance pattern in the data due to a single fault can be expressed by one eigenvector. ■

Theorem 4. Type-i fault of TE, defined in *Definition 3* by diagnostic vector $\mathbf{d}(i)$, can be described by one eigenvalue-eigenvector pair (λ_1, a_1), which has the following relations:

1. (a) $\lambda_1 = \sum_{k=1}^{3} \sigma_k^2 = \sum_{j=1}^{9} \sigma_{\chi_j}^2$ (40*a*)

   (b) $\lambda_1 = \gamma(\sigma_{\text{TE}}^F)^2 \mathbf{d}^T(i)\mathbf{d}(i)$ (40*b*)

2. $\mathbf{a}_1 = \mathbf{d}(i)$ (40*c*)

where $(\sigma_{\text{TE}}^F)^2$ is the variance of the failing tooling element TE, and γ is defined as:

$$\gamma = \frac{d(\text{CTE}, \bar{M})}{d(\text{TE}, \text{CTE})} \tag{40d}$$

where $d(\text{CTE}, \bar{M}) = \sqrt{\sum_{k=1}^{3} d^2(\text{CTE}, M_k)}$ is the average distance between sensors and CTE element.

Proof. Eq. (40a) First, it is shown that the first eigenvalue expresses the total variance of the data. Based on *Lemma,* a single type-i fault defined in Definition 3, can be expressed by one eigenvalue-eigenvector pair $(\lambda_1, \mathbf{a}_1)$. Therefore from Eq. (32), the total variance is equal to λ_1:

$$\lambda_1 = \sum_{j=1}^{9} \lambda_j = \sum_{j=1}^{9} \sigma_{\chi_j}^2 = \sigma^2 \tag{41}$$

Proof. Eq. (40b) The proof of this part is conducted only for type-1 faults. The proof for other faults can be conducted in a similar way. Substituting Eq. (40d) to Eq. (18)

$$\sigma = \sigma_{P1}^{F}\gamma \tag{42}$$

From Eq. (11)

$$\sigma_{\chi_j} = d_{1j}\sigma_{P1}^{F}\gamma \tag{43}$$

And finally, substituting Eq. (43) to Eq. (41), one can get

$$\lambda_1 = \sum_{j=1}^{9} \sigma_{\chi_j}^2 = (\sigma_{P1}^{F})^2\gamma^2 d^T(i)d(i) \tag{44}$$

Proof. Eq. (40c) By the definition of eigenvector $\mathbf{a}_1$ (Morrison, 1967) and from Eq. (31)

$$\mathbf{Q}\mathbf{a}_1 = \lambda_1\mathbf{a}_1 \tag{45}$$

The proof is only conducted for type-3 fault. The proof for other fault types can be conducted in a similar manner. From the geometrical relation of the fixture (Fig. 4) one can get

$$M_{ix} = M_i \sin\beta_i = M_i \frac{z(P_1, M_i)}{d(P_1, M_2)}; \quad M_{iy} = 0;$$

$$M_{iz} = M_i \cos\beta_i = M_i \frac{x(P_1, M_i)}{d(P_1, M_2)}, \quad i = 1, 2, 3 \tag{46}$$

Based on Theorem 2, if the pin P_2 is dislocated about ξ_{P2}, it causes part rotation with angle α, and with center of rotation around pin P_1. For small α the following relations hold:

$$M_i = d(P_1, M_i)\alpha \tag{47}$$

and

$$\xi_{P2} = d(P_1, P_2)\,\alpha \Rightarrow \alpha = \frac{\xi_{P2}}{d(P_1, P_2)} \tag{48}$$

Substituting Eq. (48) to Eq. (47)

$$M_i = \frac{d(P_1, M_i)}{d(P_1, P_2)}\xi_{P2} \tag{49}$$

Substituting Eq. (49) to Eq. (46)

$$M_{ix} = \frac{z(P_1, M_i)}{d(P_1, P_2)}\xi_{P2}; \quad M_{iy} = 0;$$

$$M_{iz} = \frac{x(P_1, M_i)}{d(P_1, P_2)}\xi_{P2}, \quad i = 1, 2, 3 \tag{50}$$

Substituting Eq. (50) to Eq. (13):

$$\chi_{(3)} = \frac{[z(P_1, M_1) \;\; 0 \;\; x(P_1, M_1) \;\; z(P_1, M_2) \;\; 0 \;\; x(P_1, M_2) \;\; z(P_1, M_3) \;\; 0 \;\; x(P_1, M_3)]^T}{d(P_1, P_2)}\xi_{P2} \tag{51}$$

which is equivalent to $\chi_{(3)} = \gamma\mathbf{d}(3)\xi_{P2}$. It can be generalized for type-i fault

$$\chi_{(i)} = \gamma\mathbf{d}(i)\xi_i \tag{52}$$

Covariance matrix $\mathbf{Q}$ of $\chi_{(3)}$ is equal to

$$\mathbf{Q} = E(\chi_{(3)}\chi_{(3)}^T) = \gamma^2 E[(\mathbf{d}(3)\xi_{P2})(\mathbf{d}(3)\xi_{P2})^T]$$
$$= \gamma^2\mathbf{d}(3)E[\xi_{P2}\xi_{P2}^T]\mathbf{d}^T(3) = \gamma^2(\sigma_{P2}^{F})^2(\mathbf{d}(3)\mathbf{d}^T(3)) \tag{53}$$

where $E[\xi_{P2}\xi_{P2}^T] = (\sigma_{P2}^{F})^2$. Based on Eq. (53)

$$Qd(3) = \gamma^2(\sigma_{P2}^{F})^2(\mathbf{d}(3)\mathbf{d}^T(3))\mathbf{d}(3) \tag{54}$$
$$= \gamma^2(\sigma_{P2}^{F})^2\mathbf{d}(3)(\mathbf{d}^T(3)\mathbf{d}(3))$$

From Eq. (44), Eq. (54) can be rearranged as

$$\mathbf{Q}\mathbf{d}(i) = \lambda_1\mathbf{d}(i) \tag{55}$$

which is equivalent to the definition of $\mathbf{a}_1$, thus $\mathbf{a}_1 = \mathbf{d}(i)$ ■

5 Fault Mapping Procedure

This section presents a procedure for mapping an unknown fault onto the variation pattern model. The mapping is realized in two steps (Fig. 5): (1) estimation of the dominant direction of the variation pattern described by one mode, and (2) fault classification of the dominant direction using a minimum distance classifier.

Estimating the dominant direction for the first dominant variation mode is realized by Criterion of Dominant Direction $C_D(1)$ defined as:

$$C_D(1) = \begin{Bmatrix} X \text{ or } Z & \text{if } c_x(1) \text{ or } c_z(i) = \max\langle c_x(1), c_y(1), c_z(1)\rangle \\ Y & \text{if } c_y(1) = \max\langle c_x(1), c_y(1), c_z(1)\rangle \end{Bmatrix} \tag{56}$$

where $c_x(1)$, $c_y(1)$ and $c_z(1)$ are:

$$c_x(1) = \sum_{j=1}^{n=9} a_{1(3j-2)}^2, \quad c_y(1) = \sum_{j=1}^{n=9} a_{1(3j-1)}^2,$$
$$c_z(1) = \sum_{j=1}^{n=9} a_{1(3j)}^2 \tag{57}$$

where a_{1i} is the ith element in the principal component a_1 obtained from PCA analysis.

This criterion can be applied because the faults in the Y axis are orthogonal to the faults in the X or Z axes. It allows simplified classification by filtering out the independent faults in the Y axis from faults in the X or Z axis. It makes classification less sensitive to errors caused by noise. This criterion allows us to focus fault classification on the dominant direction of the variation described by the following elements of the first eigenvector: in the X axis $\{a_{i1}, a_{i4}, a_{i7}\}$ or Z axis $\{a_{i3}, a_{i6}, a_{i9}\}$, and in the Y axis $\{a_{i2}, a_{i5}, a_{i8}\}$.

Having estimated the dominant direction, the fault classification is presented. The variation pattern model with defined diagnostic vectors $\{\mathbf{d}(1), \ldots, \mathbf{d}(m)\}$ describes $m = 6$ classes $\{\mathbf{D}_1, \ldots, \mathbf{D}_6\}$ of fault which need to be classified. First, a minimum distance classifier is designed (Kannatey-Asibu, 1982). Actually two classifiers will be designed: one for classification of faults in the X or Z axis, and the second one for classification in the Y axis. There are three faults in the Y axis described by $\mathbf{d}(4)$, $\mathbf{d}(5)$ and $\mathbf{d}(6)$, and three faults in the X or Z axis: $\mathbf{d}(1)$, $\mathbf{d}(2)$, and $\mathbf{d}(3)$.

Classification of Faults in the X and Z axes. Let the vector $\mathbf{a}(a_1, a_3, a_4, a_6, a_7, a_9)$ be the first principal component, which

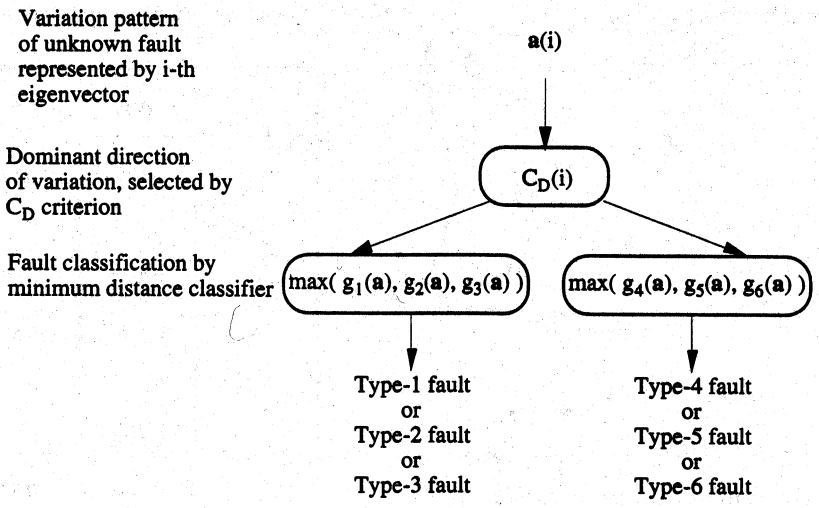

Fig. 5 Schematic diagram of fault classification procedure

describes the variation pattern of an unknown fault which needs to be classified as belonging to either $\mathbf{D}_1$, $\mathbf{D}_2$, or $\mathbf{D}_3$ (fault type-1, -2 or -3). A fault described by variation pattern a is classified into $\mathbf{D}_i$ ($i = 1, 2, 3$), if a is closest to $\mathbf{d}(i)$. Decision boundaries, which separate classes $\mathbf{D}_1$, $\mathbf{D}_2$, or $\mathbf{D}_3$, are selected perpendicular bisectors of the lines joining $\mathbf{d}(1) = [d_{11}, d_{13}, d_{14}, d_{16}, d_{17}, d_{19}]^T$, $\mathbf{d}(2) = [d_{21}, d_{23}, d_{24}, d_{26}, d_{27}, d_{29}]^T$, and $\mathbf{d}(3) = [d_{31}, d_{33}, d_{34}, d_{36}, d_{37}, d_{39}]^T$. Let $\mathrm{d}(\mathbf{a}, \mathbf{d}(i))$ denote the distance of $\mathbf{a}$ from $\mathbf{d}(i)$, where $i = 1, 2, 3$. Then

$$d^2(\mathbf{a}, \mathbf{d}(i)) = \|\mathbf{a} - \mathbf{d}(i)\|^2 = (\mathbf{a} - \mathbf{d}(i))^T(\mathbf{a} - \mathbf{d}(i))$$
$$= \|\mathbf{a}\|^2 - 2\{\mathbf{d}^T(i)\mathbf{a} - \tfrac{1}{2}\|\mathbf{d}(i)\|^2\} \quad (58)$$

Minimizing quantity $d^2(\mathbf{a}, \mathbf{d}(i))$ is equivalent to maximizing $\{\mathbf{d}^T(i)\mathbf{a} - \frac{1}{2}\|\mathbf{d}(i)\|^2\}$, where $\frac{1}{2}\|\mathbf{d}(i)\|^2$ is called the threshold of the classifier (Fukunaga, 1972). Thus, the discriminant function describing the classifier can be presented in the following way:

$$g_i(\mathbf{a}) = \{\mathbf{d}^T(i)\mathbf{a} - \tfrac{1}{2}\|\mathbf{d}(i)\|^2\}, \quad i = 1, 2, 3 \quad (59)$$

Substituting the values of $\mathbf{d}(i)$, $i = 1, 2, 3$, the individual discriminant function are obtained

$$g_i(\mathbf{a}) = d_{i1}a_1 + d_{i3}a_3 + d_{i4}a_4 + d_{i6}a_6 + d_{i7}a_7 + d_{i9}a_9 - \tfrac{1}{2}(d_{i1}^2 + d_{i3}^2 + d_{i4}^2 + d_{i6}^2 + d_{i7}^2 + d_{i9}^2),$$
$$i = 1, 2, 3 \quad (60)$$

Decision rules for 3-class minimum distance classifier can be presented as

If $g_i(\mathbf{a}) = \max(g_1(\mathbf{a}), g_2(\mathbf{a}), g_3(\mathbf{a}))$,

then $\mathbf{a} \in \mathbf{D}_i$, $i = 1, 2, 3$ (61)

Classification of faults in the Y axis. Let vector $\mathbf{a}(a_2, a_5, a_8)$ describe the variation pattern of an unknown fault which needs to be classified as belonging to either $\mathbf{D}_4$, $\mathbf{D}_5$, or $\mathbf{D}_6$ (fault type-4, -5, or -6). The fault described by variation pattern a is classified into $\mathbf{D}_i$ ($i = 4, 5, 6$), if $\mathbf{a}$ is closest to $\mathbf{d}(i)$. Let $\mathbf{d}(a, d(i))$ denote the distance of $\mathbf{a}$ from $\mathbf{d}(i)$, where $i = 4, 5, 6$. Following Eqs. (58) and (59), and substituting the values of $\mathbf{d}(i)$ for $i = 4, 5, 6$ the individual discriminant functions are obtained as

$$g_i(\mathbf{a}) = d_{i2}a_2 + d_{i5}a_5 + d_{i8}a_8 - \tfrac{1}{2}(d_{i2}^2 + d_{i5}^2 + d_{i8}^2),$$
$$i = 4, 5, 6 \quad (62)$$

Decision rules for 3-class minimum distance classifier can be presented as

If $g_i(\mathbf{a}) = \max(g_4(a), g_5(a), g_6(a))$,

then $\mathbf{a} \in \mathbf{D}_i$, $i = 4, 5, 6$ (63)

Evaluation of mapping procedure is based on the relative distance η between the unknown fault a and the closest known type-i fault, described by $d(i)$ (Table 2):

$$\eta = \frac{2\|g(\mathbf{a}) - g(\mathbf{d}(i))\|}{\|\mathbf{d}(i)\|^2} \cdot 100\% \quad (64)$$
$$= 2\|g(\mathbf{a}) - g(\mathbf{d}(i))\| \cdot 100\%$$

The correct fault classification is done when

$$\eta < \eta_0. \quad (65)$$

where η_0 depends on the variability of the fault, and was selected based on experience as $\eta_0 = 40\%$. For $\eta = 0$ the unknown fault has exactly the same variation pattern as fault estimated directly from the model of variation pattern (Table 2).

6 Simulation Results: Failure of the Locating Pin P_2 (S/N = 45 Percent Noise)

This section verifies the proposed approach through simulations. As an example, the locating pin P_2 failure is simulated by Monte Carlo approach (Rubinstein, 1981).

Methodology. In order to simulate measurement data that follows the Gaussian distribution with given mean and variance, random numbers are generated. These random numbers are substituted for part mislocation caused by a failing locating pin P_2. The range of the random numbers represents the range of part mislocation from nominal position at pin P_2. Further, for each generated random number the measurement readings from sensors 1, 2, and 3 are calculated, based on the information about location of the TE in the fixture. These numbers are substituted for sensor readings $M_1(x, y, z)$, $M_2(x, y, z)$, $M_3(x, y, z)$ producing a series of measurements, whose variation pattern follows a single fault. Fifteen simulations with 300 samples each were conducted for each case. The locating pin P_2 failure characteristics were selected as shown in Table 3.

Table 3 Characteristics of a simulated locating pin P_2 failure

Sample size	Mean [mm]	6-Sigma [mm]	Range [mm]
300	1.52	5.50	3.00

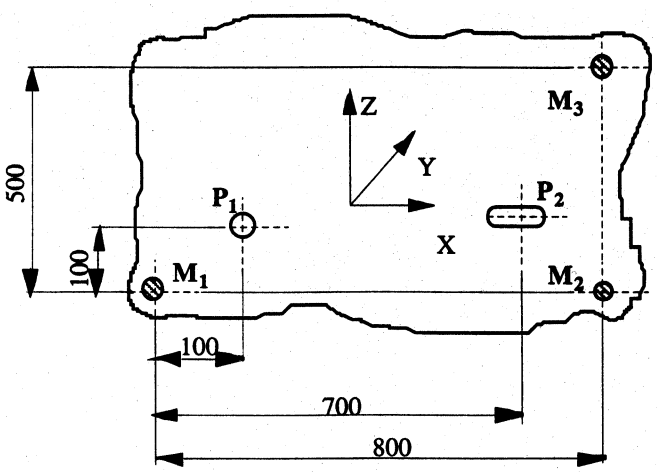

Fig. 6 The geometry of the fixture used for simulations

The model of variation pattern for the fixture (Fig. 6) is shown in Table 4.

Noise. Simulations include Gaussian additive noise, which refers to external random excitations. In the case of the autobody assembly process, additive noise is caused by: part dimensional variation due to stamping operations or clearance on the locators. Additive noise was added to all measurements with standard deviation 6-σ 2.5 mm. A random noise pattern was generated as: $M_i' = M_i + RND$, where M_i' is the ith sensor with added noise, M_i is the ith sensor without noise, and RND is a random normal deviate. To quantitatively described additive noise, the following signal-to-noise ratio is proposed:

$$\frac{S}{N} = \frac{6\sigma \text{ standard deviation of the TE fault}}{6\sigma \text{ standard deviation of the noise}} \tag{66}$$

Simulations results. Table 5 shows a dispersion report with characteristics from one batch of measurements. During PCA analysis, the Criterion of the Mode Importance (CMI) (Ceglarek et al., 1994), shows that the first dominant mode explains 94.8 percent of variation:

$$\text{CMI} = 100\,\frac{\lambda_i}{\text{trace}(\Sigma)}\,(\%) = \{94.8 \quad 5.2 \quad 0 \quad 0 \quad 0 \quad 0\} \tag{67}$$

The eigenvalue-eigenvector pair $(\mathbf{a}_1, \lambda_1)$ of the first mode is equal to:

$$\lambda_1 = 3.03; \quad a_1 = [0.150 \quad 0 \quad 0.150 \quad 0.150 \quad 0 \quad 0.585 \quad 0.406 \quad 0 \quad 0.652]^T \tag{68}$$

The average CMI for 15 independent simulations with sample of 300 is shown below:

CMI corresponding to the	mean	σ
1st mode	94.67	0.88
2nd mode	5.13	0.70

The Criterion of Dominant Direction (C_D) estimated for the first mode shows that $C_D = \{Z, c_z = \max(0.2098, 0, 0.7898)\}$.

Fault classification (Z axis). From Eq. (60) $g_3(\mathbf{a}) = \max(0.007, -0.092, 0.492) = 0.492$, showing $\eta = 1.6$ percent deviation from the single $\mathbf{d}(3)$ fault without noise. Graphically, the fault mapping mechanism is shown in Fig. 7. Simulated fault classification for all 15 batches has maximum deviation η within 1.9 percent, an average deviation 1.42 percent and 1-sigma variation of the deviation 0.21, which under the condition from Eq. (59) provides 100 percent correct diagnosis.

Table 4 Predetermined model of the variation pattern for fixture in Fig. 6

element \ vector	d(1)	d(2)	d(3)
1	0.1206	0.5774	0.0926
2	0	0	0
3	0.8427	0	0.0926
4	0.1206	0.5774	0.0926
5	0	0	0
6	0.1206	0	0.6471
7	0.4816	0.5774	0.3698
8	0	0	0
9	0.1206	0	0.6471

7 Case Study

The case study presented describes a problem which occurred during framing operations in one of the domestic assembly plants.

Problem description. A large variation was observed in the Z axis of the aperture. Figure 8 shows the aperture panel with marked measurement locations.

The model of the variation pattern for the fixture (Fig. 9) is shown in Table 6.

Estimation of the variation pattern. During PCA analysis, the CMI criterion (Ceglarek et al., 1994) shows that the first dominant mode explains 59.7 percent of variation:

$$CMI = \{59.7 \quad 24.2 \quad 9.4 \quad 4.3 \quad 1.3 \quad 1.0\} \tag{69}$$

The eigenvalue-eigenvector pair $(\mathbf{a}_1, \lambda_1)$ of the first mode is equal to:

Table 5 Dispersion report—fault of the locating pin P_2

MLP		6-Sigma [mm]
M_1	X	0.906
M_1	Z	0.906
M_2	X	0.906
M_2	Z	6.347
M_3	X	3.627
M_3	Z	6.347

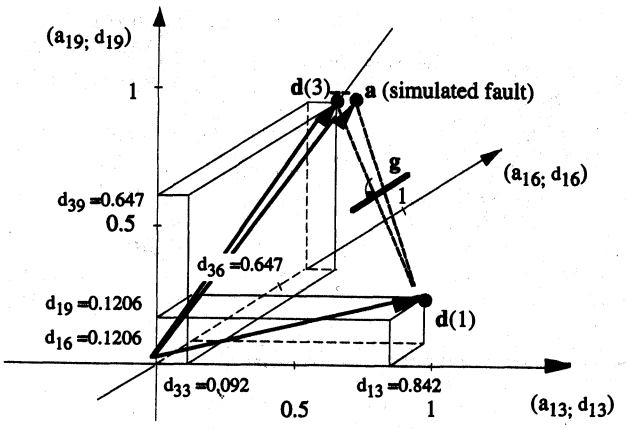

a_{13}=0.150
a_{16}=0.585
a_{19}=0.625 (Eq. 68)

d_{13}=0.842
d_{16}=0.120
d_{19}=0.647
d_{33}=0.092
d_{36}=0.647
d_{39}=0.647 (Tab. 4)

Fig. 7 Graphical representation of the fault mapping mechanism—noise 45 percent

$$\lambda_1 = 0.30; \quad \mathbf{a}_1 = [0.049 \quad 0 \quad 0.104 \quad 0.257 \quad 0 \quad 0.431 \quad 0.002 \quad 0 \quad 0.857] \quad (70)$$

The Criterion of Dominant Direction $C_D = \{Z, c_z = \max(0.0685, 0, 0.9315)\}$ shows that the Z axis is the dominant direction for the first mode.

Classification of fault in the Z axis. From Eq. (60) $g_3(\mathbf{a}) = \max(-0.244, 0.277, 0.414) = 0.414$, showing $\eta = 17.1$ percent deviation from the fault $d(3)$. Graphically, the fault mapping mechanism is shown in Fig. 10.

Conclusions. 59.7 percent of the variation in the aperture panel is caused by failure of locating pin P_2 with deviation $\eta = 17.7$ percent,

Corrective action. Locating pin P_2 was replaced in the framing station

Evaluation. On average variation was reduced around 20 percent for the analyzed sensors. The maximum variation shown by sensor $M_3(z)$ was reduced 50 percent.

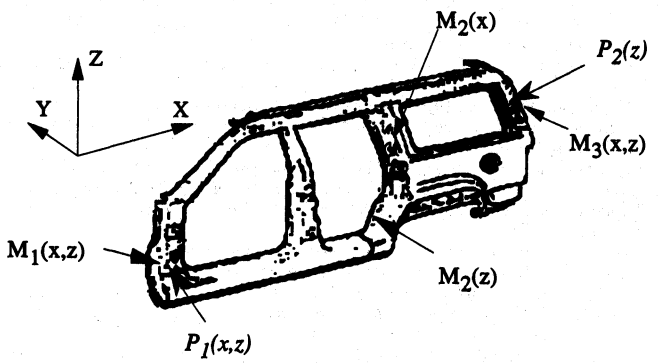

Fig. 8 Left handed aperture part with marked sensors and locating pins

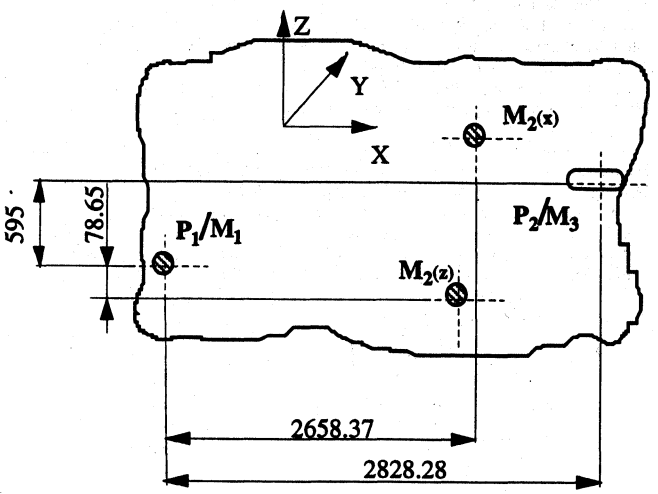

Fig. 9 Sensor location and the geometry of the fixture used in the Framing station

8 Summary and Conclusion

The complexity of the assembly line due to the number of parts and stations and its high production rate, puts high demands on the tooling equipment. Fixture failure diagnosis based on in-line measurements, is an important issue in autobody dimensional integrity.

Table 6 Predetermined model of the variation pattern for the framing station

vector / element	d(1)	d(2)	d(3)
1	0.200	0.5774	0
2	0	0	0
3	0.9515	0	0
4	0.2266	0.5774	0.0200
5	0	0	0
6	0.0572	0	0.6768
7	0	0.5774	0.1515
8	0	0	0
9	0	0	0.7201

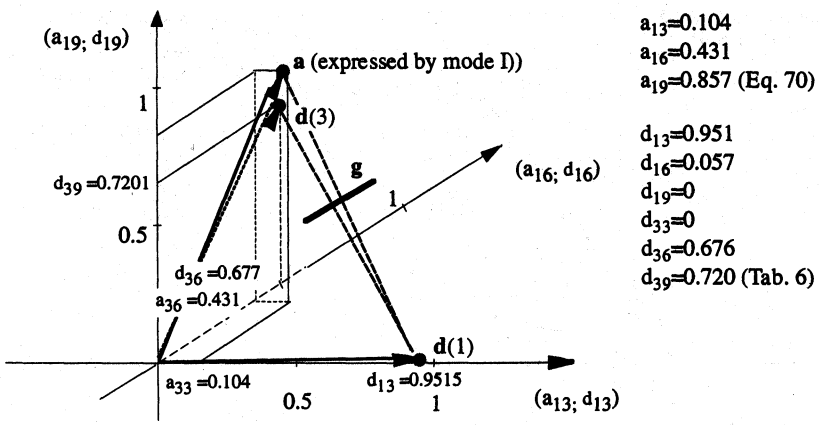

Fig. 10 Graphical representation of the fault mapping

This paper develops a fixture failure diagnostic method based on the fixture geometry and in-line measurements. The proposed solution, based on the fixture geometry and measurement locations, is generic enough to apply to multi-fixture systems such as an autobody assembly. In this paper a generic model of variation pattern for 3-2-1 fixtures and fault mapping mechanism are proposed.

The model of the variation pattern is based solely on the fixture configuration and measurement location. The relations between layout of tooling elements and measurements are developed and used for modeling of the fault variation pattern. Additionally, hypothetical tooling faults as well as their manifestation through dimensional sensors are thoroughly discussed. A major advantage of the proposed model is that the variation pattern of faults can be predetermined based only on the CAD data available during tooling design. In addition, a model can be created during the development cycle for all fixtures.

Fault mapping includes two tasks: (1) estimation of the dominant direction of the fault variation pattern, and (2) fault classification of the dominant direction using a minimum distance classifier. A minimum distance classifier determines the unknown fault based on its distance from the predetermined variation pattern described in the model. The variation pattern of the unknown fault is described through Principal Component Analysis.

The verification of the proposed method is presented through a series of computer simulations and one case study based on production data. These simulations and the one case study have demonstrated that dimensional faults can be isolated by using the proposed approach in the noisy production environment. The simulation results show that the presented approach is robust in a 45 percent noise environment.

References

ABC, 1993, "Variation Reduction for Automotive Body Assembly," Annual Report for Advanced Technology Program (NIST), Autobody Consortium (ABC) and University of Michigan, Ann Arbor.

Asada, H., and By, A., 1985, "Kinematic Analysis of Workpart Fixturing for Flexible Assembly with Automatically Reconfigurable Fixtures," *IEEE Journal of Robotics and Automation,* Vol. RA-1, No. 2, pp. 86–94.

Ceglarek, D., 1994, "Knowledge-Based Diagnosis for Automotive Body Assembly: Methodology and Implementation," Ph.D. Dissertation, University of Michigan, Ann Arbor.

Ceglarek, D., Shi, J., 1995, "Dimensional Variation Reduction for Automotive Body Assembly," *Manufacturing Review,* Vol. 8, No. 2, pp. 139–154.

Ceglarek, D., Shi, J., and Wu, S. M., 1994, "A Knowledge-based Diagnosis Approach for the Launch of the Auto-body Assembly Process," ASME JOURNAL OF ENGINEERING FOR INDUSTRY, Vol. 116, No. 3, pp. 491–499.

Ceglarek, D., Shi, J., Zhou, Z., 1993, "Variation Reduction for Body Assembly: Methodologies and Case Studies Analysis," Technical Report of the "2 mm" Program, University of Michigan, Ann Arbor.

Chou, Y-C., Chandru, V., and Barash, M. M., 1989, "A Mathematical Approach to Automatic Configuration of Machining Fixtures: Analysis and Synthesis," ASME JOURNAL OF ENGINEERING FOR INDUSTRY, Vol. 111, pp. 299–306.

Dessouky, M. I., Kapoor, S. G., and DeVor, R. E., 1987, "A Methodology for Integrated Quality System," ASME JOURNAL OF ENGINEERING FOR INDUSTRY, Vol. 109, pp. 241–247.

Faltin, F. W., and Tucker, W. T., 1991, "On-line Quality Control for the Factory of the 1990s and Beyond," In Statistical Process Control Manufacturing: J. B. Keats and D. C. Montgomery, eds., Dekker Inc.

Fukunaga, K., 1972, *Introduction to Statistical Pattern Recognition,* Academic Press, NY.

Hu, S., and Wu, S. M., 1992, "Identifying Root Causes of Variation in Automobile Body Assembly Using Principal Component Analysis," *Trans. of NAMRI,* Vol. XX, pp. 311–316.

Jolliffe, I. T., 1986, *Principal Component Analysis,* Springer-Verlag.

Kannatey-Asibu, E., 1982, "On the Application of the Pattern Recognition Method to Manufacturing Process Monitoring," *Trans. of NAMRI,* Vol. X, pp. 487–492.

Menassa, R. J., and DeVries, W. R., 1989, "Locating Point Synthesis in Fixture Design," *Annals of CIRP,* Vol. 38, No. 1, pp. 165–169.

Morrison, D. F., 1967, *Multivariate Statistical Methods,* McGraw-Hill Inc.

Paul, R., 1981, *Robot Manipulators: Mathematics, Programming, and Control,* The MIT Press.

Roan, C., Hu, S. J., and Wu, S. M., 1993, "Computer Aided Identification of Root Causes of Variation in Automobile Body Assembly," *ASME Winter Annual Meeting,* Vol. 64, pp. 391–400, New Orleans.

Rubinstein, R. Y., 1981, *Simulation and the Monte Carlo Method,* Wiley and Sons, New York.

Salisbury, J. K., and Roth, B., 1983, "Kinematic and Force Analysis of Articulated Mechanical Hands," ASME *Journal of Mechanisms, Transmissions and Automation in Design,* Vol. 105, pp. 34–41.

Shekhar, S., Khatib, O., and Shimojo, M., 1988, "Object Localization with Multiple Sensors," *The International Journal of Robotics Research,* Vol. 7, No. 6, pp. 35–44.

Schwarz, S. A., and Lu, S. C-Y., 1992, "Representation, Acquisition, and Manipulation of Probabilistic Attribute Values to Support Engineering Decision Making," *Trans of NAMRI,* Vol. XX, pp. 261–267.

Takezawa, N., 1980, "An Improved Method for Establishing the Process-Wise Quality Standard," *Rep. Stat. Appl. Res., JUSE,* Vol. 27, No. 3, pp. 63–75.

Tlusty, J., and Andrews, G. C., 1983, "A Critical Review of Sensors for Unmanned Machining" *Annals of the CIRP,* Vol. 32, pp. 563–572.